

## Polyoligopeptides functionalized zinc(II)porphyrins. Step towards artificial hemes

Shawkat M. Aly<sup>a†</sup>, Hannah Guernon<sup>a</sup>, Brigitte Guérin<sup>\*b</sup> and Pierre D. Harvey<sup>\*a◇</sup>

<sup>a</sup> *Département de chimie, Université de Sherbrooke, Sherbrooke, PQ, Canada*

<sup>b</sup> *Centre d'imagerie moléculaire de Sherbrooke (CIMS) and Département of Médecine Nucléaire et de Radiobiologie, Faculty of Medicine and Health Sciences, Université de Sherbrooke, 3001, 12<sup>e</sup> Avenue Nord, Sherbrooke, Québec J1H 5N4, Canada*

*Dedicated to Professor Karl M. Kadish on the occasion of his 65<sup>th</sup> birthday*

Received 6 May 2011

Accepted 21 May 2011

**ABSTRACT:** Two new zinc(II)porphyrin oligopeptide conjugates (zinc(II)-5,10,15,20-bis[4-(peptide)-phenyl]porphyrin (**5**) and -tetrakis[3,5-di(peptide)phenyl]porphyrin (**9**; peptide =  $-\text{CH}_2(\text{CO})\text{Gly-Phe-Ala-CNH}_2$ ) were prepared using the click chemistry with azides and ethynyl-containing precursors. The spectroscopic signature ( $S_0 \rightarrow S_1$  and transient  $T_1 \rightarrow T_n$  absorption, excitation and emission spectra) are typical for zinc(II)porphyrin and shows no perturbation upon anchoring the oligopeptides, whereas some small decreases in the photophysical parameters ( $\tau_F$  and  $\Phi_F$ ), and larger decrease in  $T_1$  lifetimes are noted, which are attributable to the known “loose bolt” effect. The structure for **9** in solution was addressed qualitatively using computer modeling and the comparison of the bimolecular fluorescence quenching rate constants between **5** and **9** using  $C_{60}$  as a photooxidative agent. While **5** exhibits a totally accessible zinc(II)porphyrin unit for a  $C_{60}$  approach, **9** shows a slower quenching rate constant meaning some steric hindrance must be present.

**KEYWORDS:** porphyrin, peptides, protein,  $C_{60}$ , fluorescence, photophysics, transient absorption spectra, electron transfer.

### INTRODUCTION

The recent design of peptide-porphyrin molecular systems is an area of large interest [1]. Investigations in the field of cell delivery or cell penetration for applications in photodynamic therapy, tumor therapy and anti-bacterial treatments, for examples, are current topics or research [2], as well as light harvesting devices and solar cells [3]. Their design also lead to nanomaterials [4] and dendrimers [5], supramolecular assemblies [6], semi-conductors [7] and materials for non-linear optics [8]. Studies for

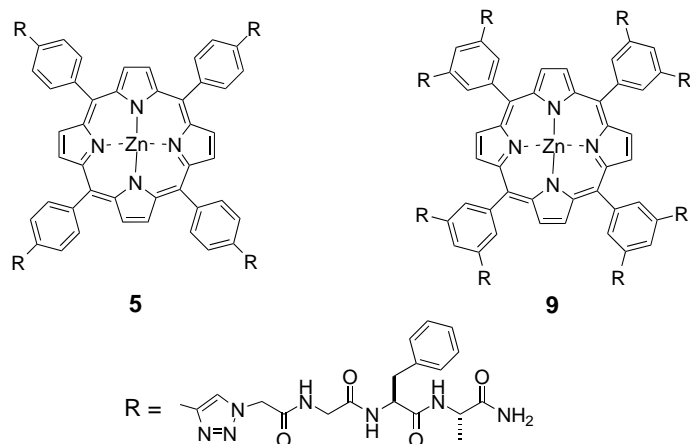
fast kinetics in the upper excited states [9] and exciton couplings [10] were also the subjects of recent interest.

The porphyrin functionalization by oligopeptides using click chemistry was recently reported by another group [11], with the purpose to render the porphyrin chromophore water soluble. This methodology is convenient and very popular nowadays. We now wish to report the synthesis of two new examples (Scheme 1). It will be shown that the spectral signature ( $S_0$ - $S_1$  and  $T_1$ - $T_n$  absorption, excitation, emission spectra) is not influenced by the functionalization of the zinc(II)porphyrin chromophore by oligopeptides but the photophysical properties of the singlet state are slightly affected whereas the triplet state is quenched by a factor of  $\sim 2$ . Finally, computer modeling and bimolecular fluorescence quenching experiments using  $C_{60}$  as an photo-oxidative agent indicate that **9** exhibits a relatively sterically hindered pocket above and below the macrocycle for a  $C_{60}$  approach.

◇SPP full member in good standing

\*Correspondence to: Pierre D. Harvey, email: Pierre.Harvey@USherbrooke.ca, tel: +1 819-821-7092, fax: +1 819-821-8017 and Brigitte Guérin, email: Brigitte.Guérin2@USherbrooke.ca

†On leave from Chemistry Department, Faculty of Science, Assiut University, Assiut, Egypt



Scheme 1. Drawings of the target molecules

## EXPERIMENTAL

### General methods

All chemicals and solvents (reagent grade) were used as supplied from the vendors cited below without further purification, unless otherwise noted. NovaSyn® TGR resin was obtained from NovaBiochem®. Fmoc-protected amino acids were obtained from EMD NovaBiochem® (Gibbstown, NJ, USA) or Chem-Impex International Inc. (Wood Dale, IL, USA). 2-(1H-7-azabenzotriazol-1-yl)-1,1,3,3-tetramethyluronium hexafluorophosphate (HATU) was purchased from Chem-Impex International Inc. All reactions requiring anhydrous conditions were conducted under a positive nitrogen atmosphere in oven-dried glassware using standard syringe techniques. Tetrahydrofuran (THF) was distilled from sodium/benzophenone immediately prior to use. Dichloromethane, ether, *N,N*-diisopropylamine (*i*-Pr<sub>2</sub>NH) and *N,N,N*-triethylamine (Et<sub>3</sub>N) were freshly distilled from CaH<sub>2</sub> under N<sub>2</sub> atmosphere. Methanol (MeOH) was distilled over Mg<sup>0</sup>/I<sub>2</sub> and stored over Type 4 Å molecular sieves. Flash chromatography was performed on Silicycle silica gel 60 (0.040–0.063 mm) using nitrogen pressure. Analytical thin-layer chromatography (TLC) was carried out on precoated (0.25 mm) Merck silica gel F-254 plates.

### Preparation of starting materials

The preparation and characterization data of **1a** [12a], **1b** [12b], **2** [12a], **3** [12a] and **4** [12a] have been reported previously.

**5,10,15,20-tetrakis[3,5-di(trimethylsilylethynyl)phenyl]porphyrin 6.** To a solution of 3,5-di(trimethylsilylethynyl)benzaldehyde **1b** (1.83 g, 6.13 mmol) in warm propionic acid (20 mL) was added the pyrrole (0.43 mL, 6.13 mmol). The resultant solution was stirred 3 h at reflux and then cooled to room temperature for 24 h. The mixture was filtered over a Buchner funnel and the residue was successively rinsed with propionic acid, water and MeOH. The solid was dried in the oven at 120 °C

for 1 h to yield 406 mg of porphyrin **6** (19%) as a purple solid. *R<sub>f</sub>* 0.45 (DCM-hexanes, 20:80). <sup>1</sup>H NMR (300 MHz, CDCl<sub>3</sub>): δ, ppm 8.83 (s, 8H), 8.23 (s, 8H), 8.03 (s, 4H), 0.26 (s, 72H), -2.97 (s, 2H).

**Zinc 5,10,15,20-tetrakis[3,5-di(trimethylsilylethynyl)phenyl]porphyrin 7.** To a solution of porphyrin **6** (400 mg, 0.289 mmol) in dry CH<sub>2</sub>Cl<sub>2</sub> (60 mL) were added Zn(OAc)<sub>2</sub> (95 mg, 0.434 mmol) in MeOH (3 mL) and Et<sub>3</sub>N (1 mL). After stirring the resultant solution for 5 h at reflux, the crude product was poured into water and extracted with 3 × 100 mL CH<sub>2</sub>Cl<sub>2</sub>, the organic extracts were combined, dried (MgSO<sub>4</sub>), filtered, and concentrated. After concentration, the desired porphyrin **7** was purified by flash chromatography on silica gel using 20% CH<sub>2</sub>Cl<sub>2</sub> in hexane to give 397 mg (95%) as a purple solid. *R<sub>f</sub>* 0.33 (DCM-hexane, 20:80). <sup>1</sup>H NMR (300 MHz, CDCl<sub>3</sub>): δ, ppm 8.91 (s, 8H), 8.24 (d, 8H, *J* = 1.4 Hz), 8.03 (t, 4H, *J* = 1.4 Hz), 0.26 (s, 72H).

**Zinc 5,10,15,20-tetrakis[3,5-di(ethynyl)phenyl]porphyrin 8.** To a solution of silylated porphyrin **7** (397 mg, 0.274 mmol) in CHCl<sub>3</sub> (20 mL) was added a 1.0 M solution TBAF in THF (4.4 mL). The resultant solution was stirred 4 h at room temperature. The reaction mixture was poured into water and extracted with 3 × 50 mL CH<sub>2</sub>Cl<sub>2</sub>, the organic extracts were combined, dried (MgSO<sub>4</sub>), filtered, and concentrated. After concentration, the desired porphyrin was purified by flash chromatography on silica gel using 20% CH<sub>2</sub>Cl<sub>2</sub> in hexane, and then with THF to give 150 mg (63%) of **8** as a purple solid. *R<sub>f</sub>* 0.38 (DCM-hexane, 60:40). <sup>1</sup>H NMR (300 MHz, CDCl<sub>3</sub>): δ, ppm 8.95 (s, 8H), 8.32 (s, 8H), 8.06 (s, 4H), 3.19 (s, 8H). HRMS (ESI): *m/z* calcd. for C<sub>60</sub>H<sub>29</sub>N<sub>4</sub>Zn [M + H]<sup>+</sup>: 869.16602; found 869.16782 (Δ = 2.07 ppm).

**Peptide.** The peptide (called **Peptide**) was synthesized by continuous flow method on a Pioneer Peptide Synthesis System (PerSeptive Biosystems) using the Fmoc strategy. A 2-fold excess of Fmoc-protected amino acids over resin substitution rate was used for coupling. Synthesis was performed using amine free DMF. Fmoc-protected amino acids were activated for coupling with an equimolar amount of HATU, and 2 equivalents of DIEA. Fmoc deprotection was performed in 20% piperidine in DMF and monitored through a UV detector at 364 nm. After the last coupling, the peptide on resin was bromoacetylated by the method of Robey [13]. At 0 °C, the bromoacetic acid (5 equiv.) was dissolved in 2 mL of CH<sub>2</sub>Cl<sub>2</sub> and EDC (2.5 equiv.) was added to the cold solution. After 15 min of stirring, the mixture was diluted in 2 mL of DMF and added to the peptide on resin pre-swelled with DCM. After 60 min of coupling, the resin was washed with DMF (3 ×), MeOH (3 ×), DMF (3 ×), MeOH (3 ×) and CH<sub>2</sub>Cl<sub>2</sub> (3 ×). The azido group was introduced by treating the bromoacetylated peptide on resin with a solution of sodium azide (5.2 equiv.) in

DMSO. For this reaction, a mechanical agitation was maintained for 24 h at room temperature. The resin was washed with DMSO (3 ×), CH<sub>2</sub>Cl<sub>2</sub> (3 ×), MeOH (3 ×) and the Kaiser's test (colorimetric reaction between resin and ninhydrine) indicated the absence of primary amines (yellow beads). The azido peptide was deprotected and cleaved from the polymer support by treatment with a cocktail of TFA:H<sub>2</sub>O:thioanisole (92:2:6, v/v) for 4 h at room temperature under a mechanical agitation. The resin was removed by filtration and washed with TFA. Combined filtrates were added dropwise to a cold ethyl ether (1 mL of TFA/10 mL of ether). The precipitated peptide was centrifuged at 1200 rpm for 25 min. The ether solution was decanted and the jelly solid was purified by using Flash chromatography on a Biotage SP4 system and a C<sub>18</sub> column. The purity of the peptide was verified by HPLC and the identity was confirmed by MS spectrometry on an API 3000 LC/MS/MS. Analytical HPLC was performed on an Agilent 1200 system equipped with a Zorbax Eclipse XDB C<sub>18</sub> reverse phase column (4.6 × 250 mm, 5 μ) and Agilent 1200 series diode array UV-vis detector. Linear gradient of 0% to 100% acetonitrile in water with 0.1% TFA in 30 min was used. The flow rate was 1 mL/min. Product purity was confirmed to be > 99% by the analytical scale reversed-phase HPLC. The average retention time is 13.0 min. MS calcd. 375.4; found 398 [M + 23 (Na)], 376 [M + 1], 359 [M - NH<sub>3</sub>], 331 [M - N<sub>3</sub>], 288 [M - Ala].

**General procedure for the preparation of porphyrin-peptide conjugates.** The porphyrin-peptide conjugates were synthesized using the procedure described by Marik [14]. To a solution of tripeptide **Peptide** (19.4 mg, 0.052 mmol) in a mixture of H<sub>2</sub>O:DMF 1:4 (100 μL:400 μL) were successively added *N,N*-diisopropylethylamine (DIPEA) (225 μL, 1.29 mmol), pyridine (52 μL, 0.65 mmol), sodium ascorbate (256 mg, 1.29 mmol), and copper iodide (24.6 mg, 0.129 mmol). A solution of the suitable porphyrin (4, 0.25 equiv. or 8, 0.13 equiv.) in DMF (300 μL) was added to the reaction mixture. The resultant solution was stirred 16 h at room temperature and then filtered on a Sepak-C<sub>18</sub> cartridge (Waters). The resulting solution was added to a cold ethyl ether. The precipitated purple compound was centrifuged at 1200 rpm for 25 min. The ether solution was decanted and the solid was purified by using Flash chromatography on a Biotage SP4 system and a C<sub>18</sub> column. The reaction mixture was poured into water. Peptide purification was done by Flash chromatography on a Biotage SP4 system using a C<sub>18</sub> column. Analytical HPLC was performed on WatersTM 600 instrument (using a 3.9 mm × 150 mm C-18 column, H<sub>2</sub>O/CH<sub>3</sub>CN as eluents, and a WatersTM 996 photodiode array detector). Linear gradient of 0% to 100% acetonitrile in water with 0.1% TFA in 30 min was used. The flow rate was 1 mL/min.

**Porphyrin-peptide conjugate 5.** The product **5** was obtained as a purple solid, 150 mg (63%). Product

purity was confirmed to be > 99% by the analytical scale reversed-phase HPLC. The average retention time is 18.0 min. MS (LC-MSD TOF): *m/z* (ESI) 1138.42 [M + 2H]<sup>2+</sup>, 1149.41 [M + H + Na]<sup>2+</sup>, 1160.41 [M + 2Na]<sup>2+</sup>. HRMS (ESI): *m/z* calcd. for C<sub>116</sub>H<sub>114</sub>N<sub>32</sub>O<sub>16</sub>Zn [M + 2H]<sup>2+</sup>: 1137.4186; found 1137.4238.

**Porphyrin-peptide conjugate 9.** Conjugate **9** was poorly soluble in HPLC solvents tested. Purification by trituration in water and different organic solvents (Et<sub>2</sub>O, CH<sub>3</sub>CN, MeOH) gave **9** as a purple solid, 23 mg (52%). Product identification and purity was confirmed by HRMS. HRMS (MALDI-TOF): *m/z* calcd. for C<sub>188</sub>H<sub>196</sub>N<sub>60</sub>O<sub>32</sub>Zn [M]<sup>+</sup>, 3869.4840; found 3869.4951 (Δ is 2.87 ppm).

## Instrumentation

Melting points were determined on an electrothermal melting point apparatus and are uncorrected. <sup>1</sup>H NMR spectra were recorded on a Bruker AC-300 NMR spectrometer using CDCl<sub>3</sub> (δ = 7.26 ppm) or DMSO (δ = 2.49 ppm) as the reference. <sup>13</sup>C NMR spectra were recorded at 75 MHz using CDCl<sub>3</sub> (δ = 77.1 ppm) as the reference. Analytical HPLC was performed on an Agilent 1200 system equipped with a Zorbax Eclipse XDB C<sub>18</sub> reverse phase column (4.6 × 250 mm, 5 μ) and Agilent 1200 series diode array UV-vis detector. Linear gradient 50% acetonitrile in water with 0.1% TFA in 40 min. The flow rate was 1 mL/min. Mass spectra were obtained on a MALDI mass spectrometry using Micro-mass TOF Spec 2F or on a LC-MSD TOF (ESI) Agilent Technologies high resolution from the Centre Régional de Spectrométrie de Masse de l'Université de Montréal or on a Bruker Ultraflex II instrument in MALDI-TOF reflectron mode using dithranol (1,8-dihydroxy-9-[10H]-anthracene) as a matrix. The UV-visible spectra were recorded on a Varian Cary 1 spectrophotometer or on a Hewlett-Packard diode array model 8452A. The emission spectra were obtained using a double monochromator Fluorolog 2 instrument from Spex. The emission lifetimes were measured on a TimeMaster Model TM-3/2003 apparatus from PTI. The source was nitrogen laser with high-resolution dye laser (FWHM ~1.4 ns) and the fluorescence lifetimes were obtained from deconvolution or distribution lifetimes analysis. The uncertainties were about 50–100 ps. The flash photolysis spectra and the transient lifetimes were measured with a Luzchem spectrometer using the 355 nm line of a YAG laser from Continuum (Serulite), and the 530 nm line from Optical Parametric Oscillator (OPO) module pump by the same laser (FWHM = 13 ns).

## Quantum yields

Measurements of quantum yields were performed in 2MeTHF at 298 K. Three different measurements (*i.e.* different solutions) were prepared for each photophysical datum (quantum yields and lifetimes). For 298 K

measurements samples were prepared under inert atmosphere (in a glove box,  $P_{O_2} < 25$  ppm). The sample and standard concentrations were adjusted to obtain an absorbance of 0.05 or less. This absorbance was adjusted to be the same as much as possible for the standard and the sample for a measurement. Each absorbance value was measured five times for better accuracy in the measurements of the quantum yields. The references used for quantum yield was Zn(TPP) (TPP = tetraphenylporphyrin;  $\Phi = 0.033$ ) [15].

### Modelization

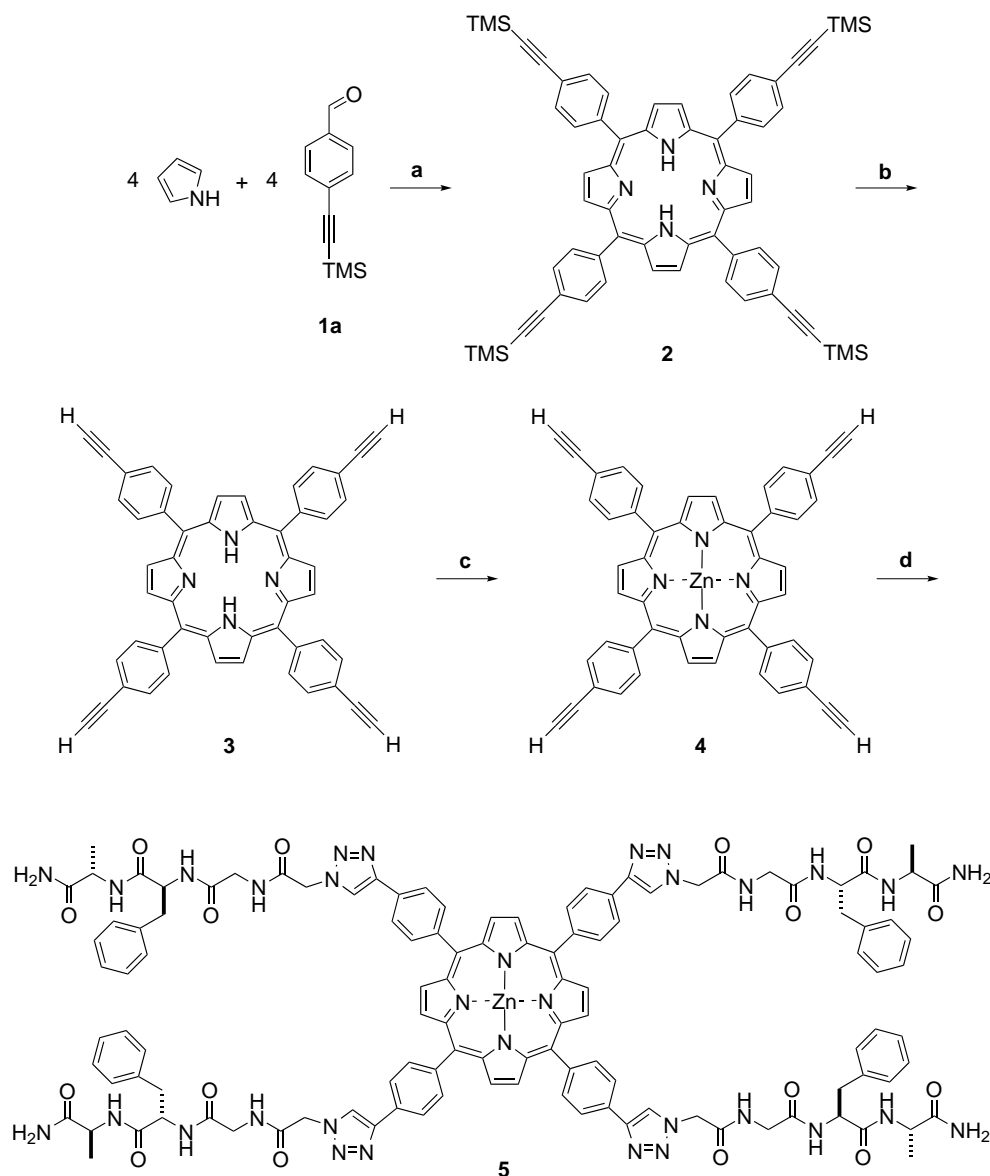
The computer modelings were performed using PCMODEL v9.2 from Serena Software (St. Louis). No constraint was applied upon energy minimization.

## RESULTS AND DISCUSSION

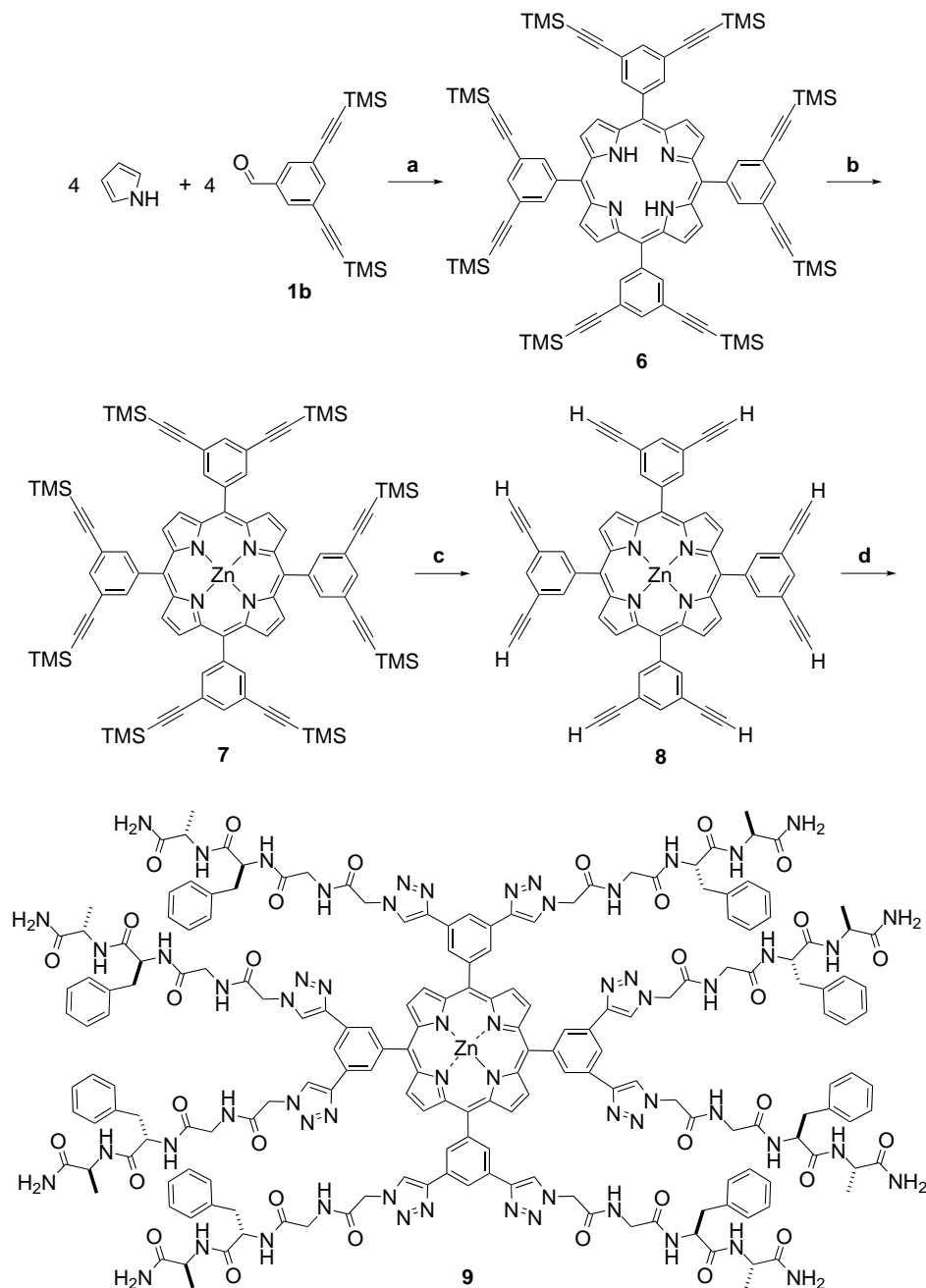
### Synthesis

The syntheses of the target conjugate compounds, **5** and **9**, are described in Schemes 2 and 3, respectively.

The synthesis steps are all standards first consisting of a condensation of a *para*- or *meta*-disubstituted benzaldehyde by ethynyltrimethylsilane with unsubstituted pyrrole in an acidic medium to generate the expected products **2** and **6**, respectively. The sequence of steps differs for the synthesis of the precursors **4** (deprotection of the ethynyltrimethylsilane then metalation) and **8** (metalation then deprotection of the ethynyltrimethylsilane). We find the reported sequence gave better yields. Compound **4** was



**Scheme 2.** (a)  $C_2H_3CO_2H$  at reflux 3 h, then at  $25^\circ C$ , 24 h; (b) TBAF 1 M in THF (10 equiv.),  $CHCl_3$ ,  $25^\circ C$ , 24 h; (c)  $Zn(OAc)_2$  (1.5 equiv.), in MeOH,  $CH_2Cl_2$ ,  $Et_3N$  (excess), reflux 16 h; (d)  $(N_3-CH_2-CO)Gly-Phe-Ala-CONH_2$  (0.052 mmol),  $H_2O:DMF$  (1:4, 500 mL), DIEA (25 equiv.), pyridine (12.5 equiv.), sodium ascorbate (25 equiv.), CuI (2.5 equiv.), then **4** (0.25 equiv.) in DMF (300 mL), stirred 16 h at  $25^\circ C$



**Scheme 3.** (a)  $C_2H_5CO_2H$  at reflux 3 h, then at 25 °C, 24 h; (b)  $Zn(OAc)_2$  (1.5 equiv.), in MeOH,  $CH_2Cl_2$ ,  $Et_3N$  (excess), reflux 5 h; (c) TBAF 1 M in THF (10 equiv.),  $CHCl_3$ , 25 °C, 24 h; (d)  $(N_3CH_2-CO)Gly-Phe-Ala-CONH_2$  (0.046 mmol),  $H_2O:DMF$  (1:4, 500 mL), DIEA (25 equiv.), pyridine (12.5 equiv.), sodium ascorbate (25 equiv.),  $CuI$  (2.5 equiv.), then **8** (0.13 equiv.) in DMF (300 mL), stirred 16 h at 25 °C

previously reported by Gerard van Koten and collaborators [12] and our results agree with theirs. Porphyrins were functionalized by conjugation with peptide moieties following the procedure described by Marik [14]. Reaction conditions have been optimized by monitoring the formation of the conjugate **5** on analytical reversed-phase HPLC. These two zinc(II)porphyrin oligopeptide conjugates were prepared with overall yields of 52–63%. The purity of porphyrin-peptide **5** was shown to be > 99% (analytical HPLC) and its identification was done using

LC-MSD TOF (ESI). Identification of porphyrin peptide conjugate **9** was done by High Resolution Mass Spectroscopy on a Bruker Ultraflex II instrument.

### Spectroscopy and photophysics

The absorption, excitation and emission spectra of **4**, **5**, **8** and **9** in DMF at 77 and 298 K are presented in Figs 1 and 2, and Table 1. The spectra were checked for molecular aggregation upon cooling at various concentrations.

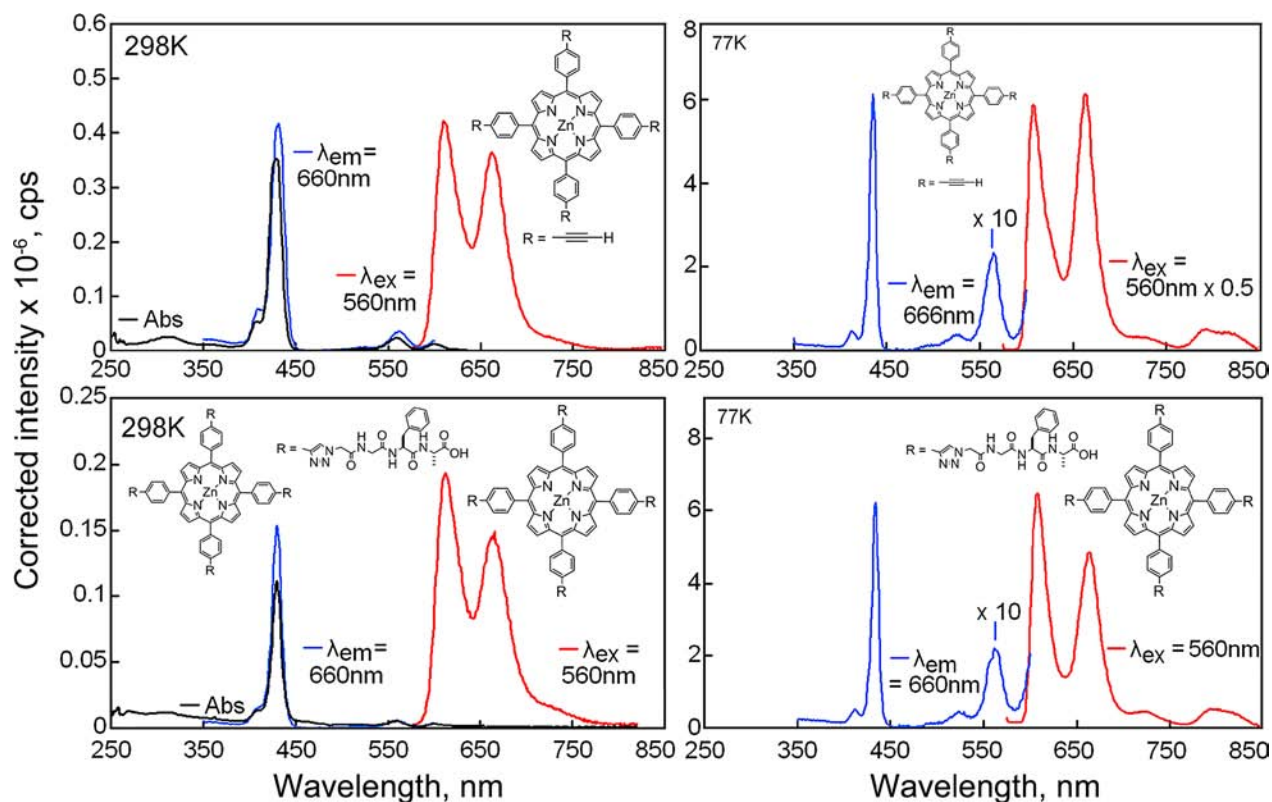


**Fig. 1.** Absorption (black), excitation (blue) and emission (red) spectra of **4**, and **5**, in DMF at 77 and 298 K. The excitation spectra cannot exceed 610 nm on our instrument

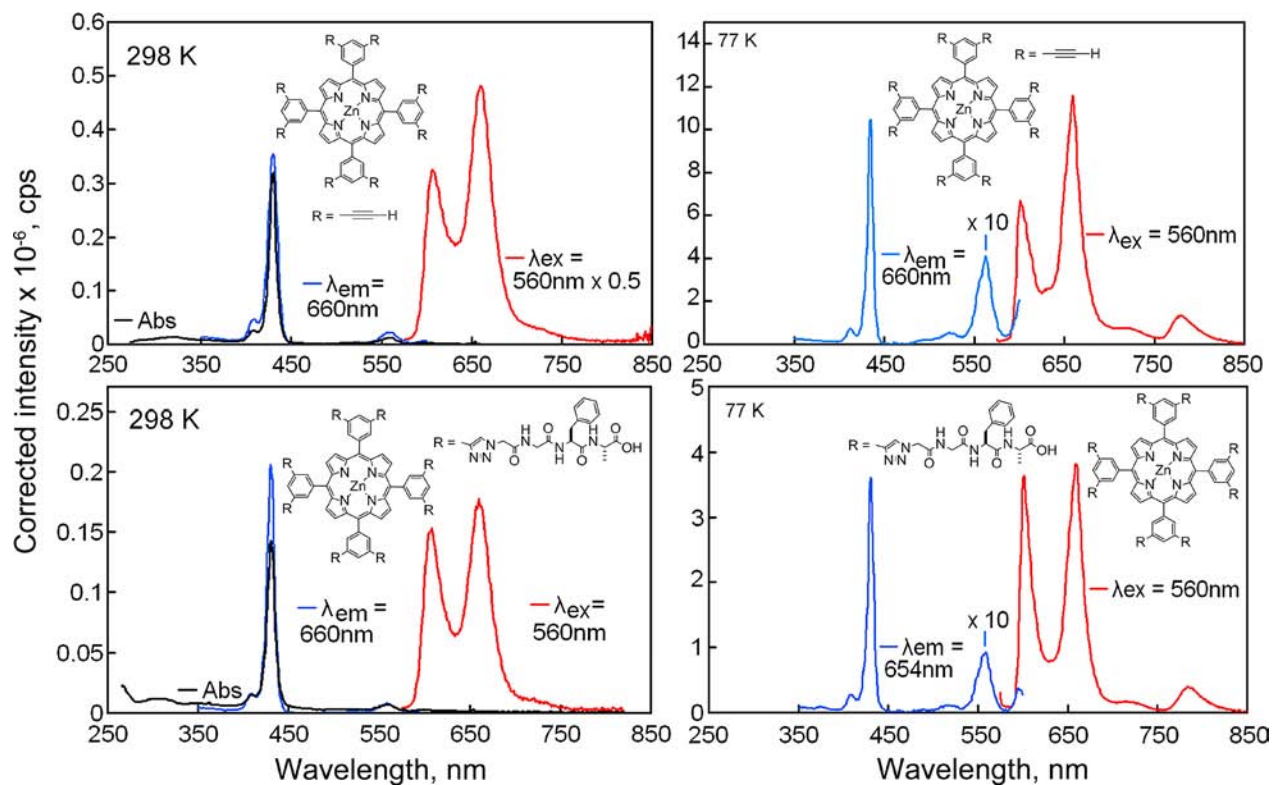


**Fig. 2.** Absorption (black), excitation (blue) and emission (red) spectra of **8**, and **9**, in DMF at 77 and 298 K. The excitation spectra cannot exceed 610 nm on our instrument

**Table 1.** Spectroscopic data for **4**, **5**, **8** and **9** in DMF

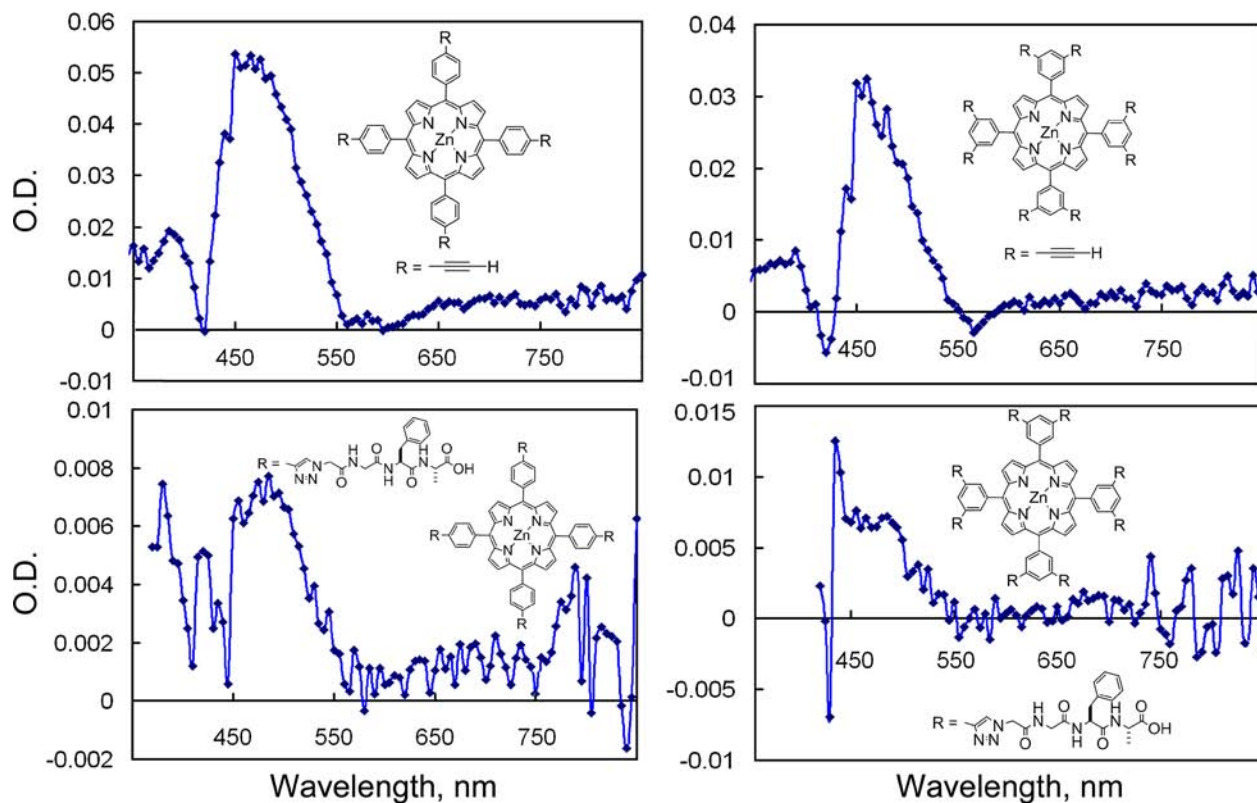
	298 K		77 K
	Abs	Fluorescence	Fluorescence
<b>4</b>	410, 430, 560, 605	611, 665	609, 665, 730sh, 795
<b>5</b>	412, 430, 562, 598	610, 660	602, 660, 722sh, 780
<b>8</b>	408, 430, 560, 605	614, 666	609, 665, 726sh, 797
<b>9</b>	412, 430, 560, 602	610, 662	602, 661, 723sh, 786

Sh = shoulder.

The excitation and fluorescence spectra did not change upon changing the concentration. The spectral signature at 77 and 298 K (*i.e.* the Soret and Q-bands in the absorption and excitation spectra, as well as the fluorescence and phosphorescence spectra) of precursor **4** vs. target **5** and

of precursor **8** vs. target **9** is almost identical in all cases. This demonstrates that the anchoring of the oligopeptides onto the *meso*-phenyl groups by the click chemistry has very little influence on the spectra and therefore the energy level, meaning that no major distortion, if any, of the chromophoric core occurs. This observation is also true for the  $T_1$ - $T_n$  transient absorption spectra (Fig. 3). The transient absorption maxima are depicted at ~540 (for **4** and **5**) and ~530 nm (for **8** and **9**) and are consistent with other examples reported in the literature for similar derivatives (transient absorption maximum located at ~500 nm) [16].

The photophysical data are presented in Table 2. The investigated species (**4**, **5**, **8** and **9**) exhibit similar and relatively low fluorescence quantum yields ( $\Phi_F$ ) and lifetimes ( $\tau_F$ ) at 298 K. On the other hand, at 77 K,  $\tau_F$  increases to  $\sim 2.0 \pm 0.5$  ns, a range that is typical for zinc(II)porphyrin chromophores [17].

**Fig. 3.** Transient absorption spectra of **4**, **5**, **8** and **9** in DMF at 298 K using  $\lambda_{exc} = 355$  nm (20 mJ per pulse) recorded right away after excitation (delay time = 0  $\mu$ s)**Table 2.** Photophysical parameters for **4**, **5**, **8** and **9** in DMF

	77 K		298 K		$\Phi_F$	$k_F$ , ns <sup>-1</sup>	$k_{nr}$ , ns <sup>-1</sup>	$\tau(T_1)$ , $\mu$ s
	$\lambda_{em}$	$\tau_F$ , ns	$\lambda_{em}$	$\tau_F$ , ns				
<b>4</b>	607	$2.56 \pm 0.15$	610	$0.59 \pm 0.07$	0.025	0.042	1.65	287
<b>5</b>	607	$2.17 \pm 0.14$	610	$0.45 \pm 0.03$	0.022	0.049	2.17	127
<b>8</b>	607	$2.37 \pm 0.03$	610	$0.52 \pm 0.02$	0.024	0.046	1.88	460
<b>9</b>	607	$1.66 \pm 0.16$	610	$0.43 \pm 0.03$	0.019	0.044	2.28	270

<sup>a</sup> The uncertainties are  $\pm 10\%$ . <sup>b</sup> The uncertainties are  $\sim \pm 10$   $\mu$ s.

Excluding the uncertainties, a slight decrease in  $\tau_F$  and in  $\Phi_F$  is observed going from **4** to **5** and from **8** to **9**. This behavior reflects the known “loose bolt” effect upon increasing the size of the substituents around aromatic chromophores [18]. Indeed, the fluorescence rate constants,  $k_F$ , ( $\Phi_F/\tau_F$ ) are found, as expected, to be relatively constant from one complex to the other, but not the non-radiative ones,  $k_{nr}$ , ( $(1 - \Phi_F)/\tau_F$ ), which show a clear increase upon the addition of the peptides. This behavior is also noted for the triplet transient lifetimes, except that the trend is more pronounced. This is explained by the fact the triplet lifetime is longer and therefore more likely to be depicted.

### Computer modeling

Modeling was performed on **9** in order to get some information on its possible structure in solution. Several

starting positions of the oligopeptides relative to the zinc(II)porphyrin central chromophore were investigated. Three of them were considered: **Conformer 1** (oligopeptides placed straight up and down with respect to the porphyrin plane;  $D_{4d}$  point group), **Conformer 2** (oligopeptides placed parallel to the porphyrin plane;  $D_{4d}$  point group when idealized) and **Conformer 3** (neighboring oligopeptides placed on top of each other to favor H-bondings;  $D_{4d}$  point group) and are shown in Figs 4–7. **Conformer 1** exhibits 4 non interacting oligopeptides after energy minimization ( $\sim 400$  kcal.mol<sup>-1</sup>), and has the highest energy of the three. Because some minor resulting structural deviations from the ideal  $D_{4d}$  point group geometry, the computed minimum energy varies a little bit from trial to trial. **Conformer 2** exhibits two H-bonding interactions between the peptide branches after minimization and has a lower energy ( $\sim 350$  kcal.mol<sup>-1</sup>)

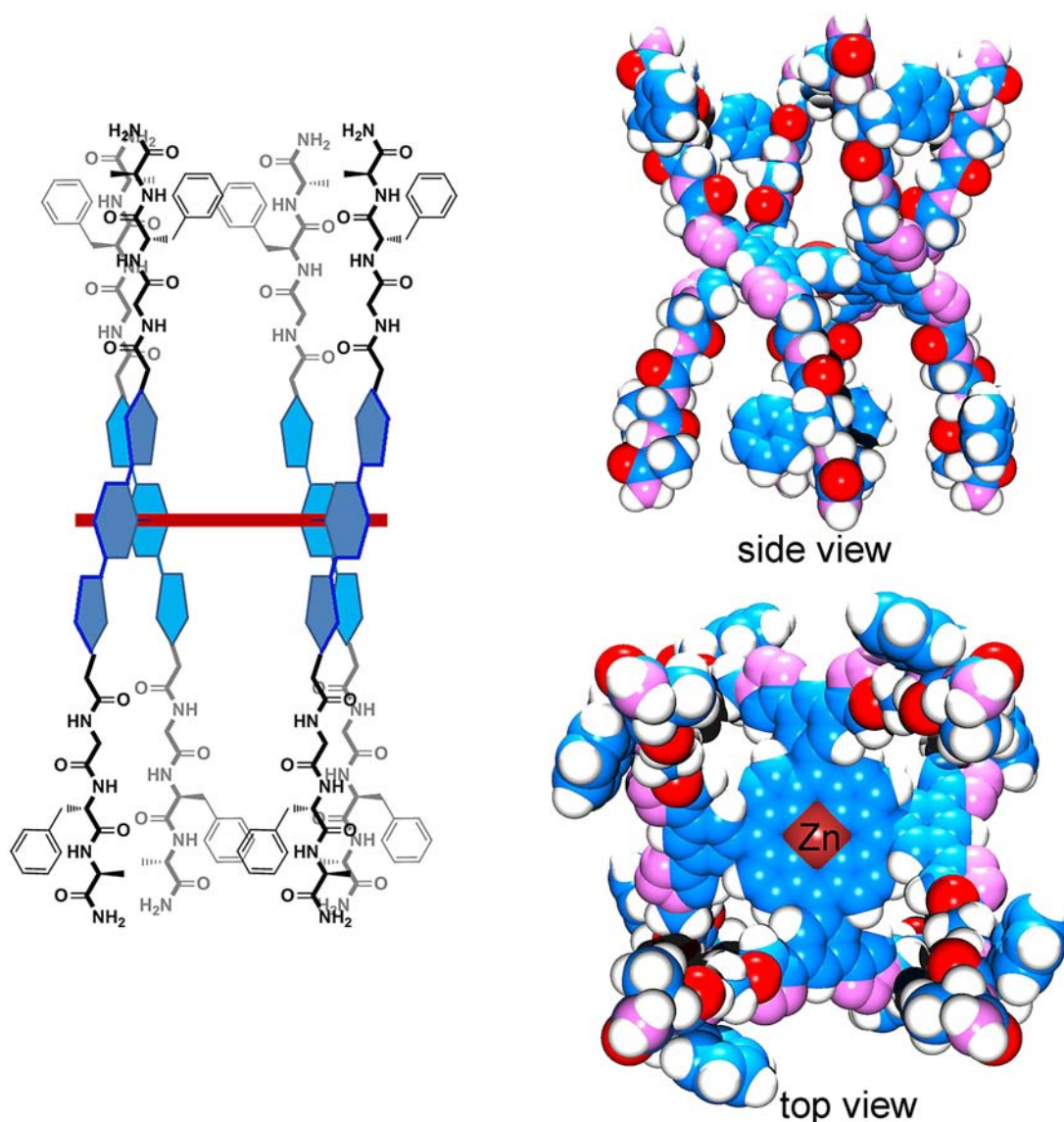


**Fig. 4.** Energy minimized geometry of **9** as **Conformer 1**. Left: scheme showing the peptides with respect to the plane. Right: side and top views of the space filling representations of the energy minimized geometry of **9**

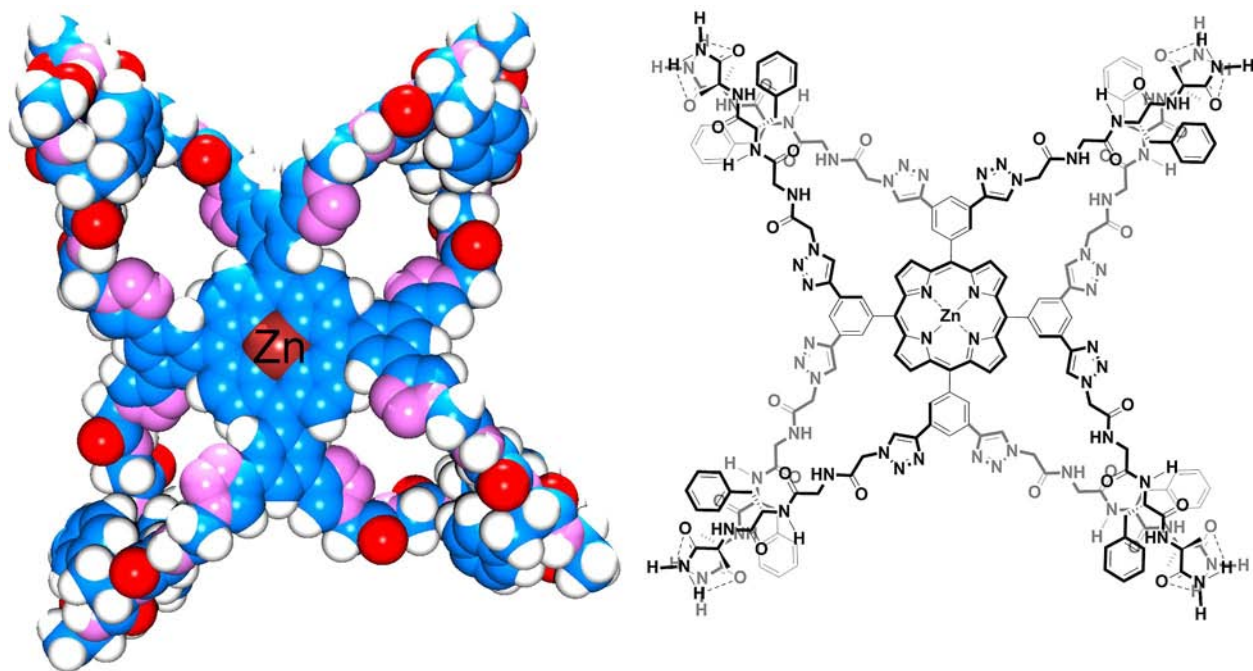


**Fig. 5.** Energy minimized geometry of **9** as **Conformer 2**. Left: top views of the space filling representation of the energy minimized geometry of **9**. Right: scheme showing the peptides with respect to the plane

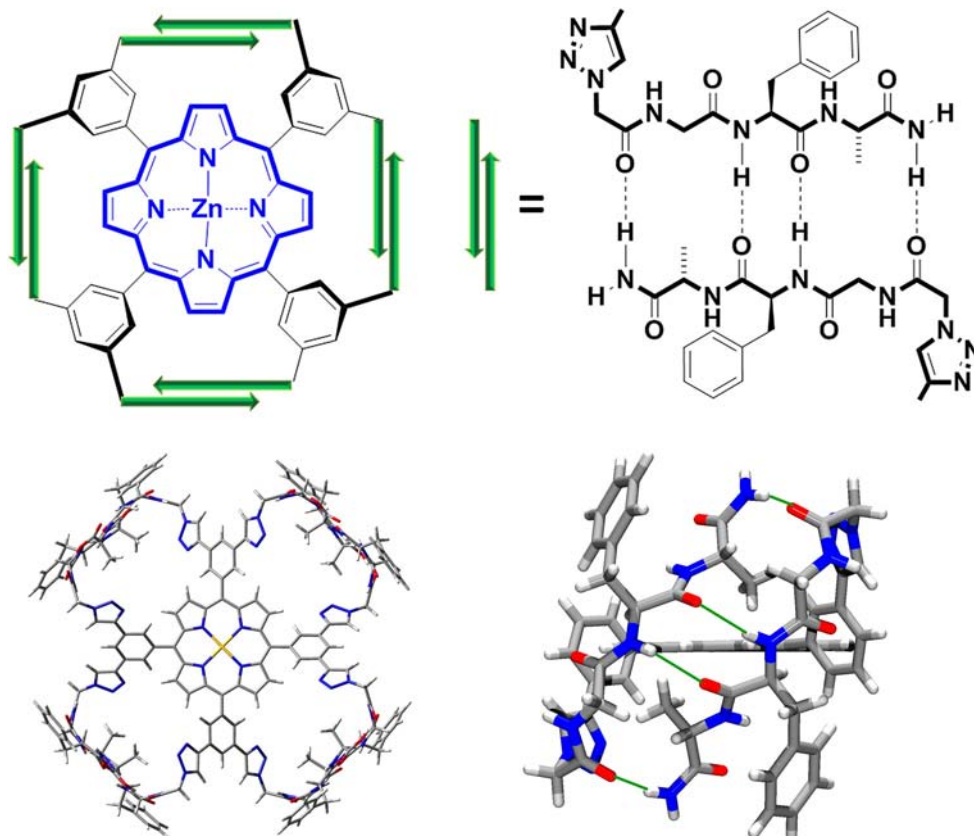


**Fig. 6.** Top left: scheme showing the relative orientation of the peptides relative to the porphyrin plane in **Conformer 3**. Top right: Chemdraw® showing the inter oligopeptide H-bonds in **Conformer 3**. Bottom left: stick representation of **9** (**Conformer 3**) in its lowest energy conformation. Bottom right: side view of this stick representation showing only one pair of interacting oligopeptides stressing the presence of H-bonds

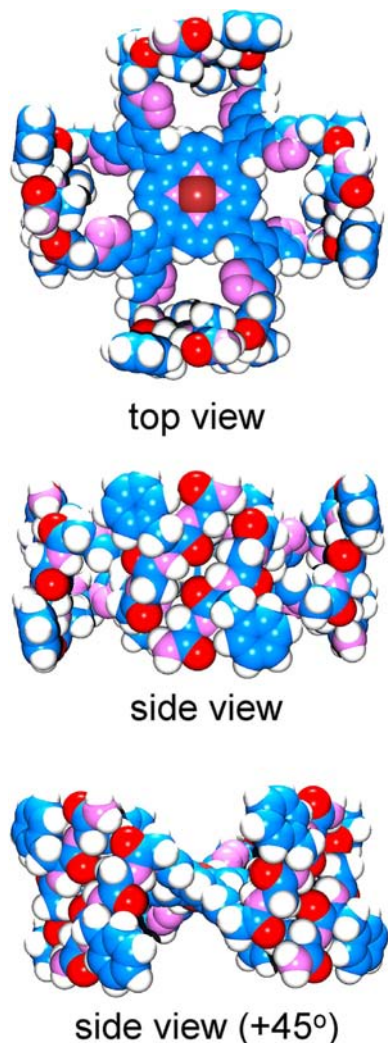


**Fig. 7.** Top: Top view of the space filling representation of **9** (**Conformer 3**) in its lowest energy conformation. Bottom: side view of this space filling representation. The two representations are turn by 45° from each other

than that for **Conformer 1**. This decrease in total energy is due to the formation of the inter-peptidic H-bonds (8 in total).

Based on this observation, **Conformer 3** was also investigated. In this case, the total energy of the molecule drops drastically ( $\sim 320$  kcal.mol<sup>-1</sup>) and is the lowest energy conformation found with 16 H-bonds formed. Globally, we reproducibly find that  $E(\text{Conformer 1}) > E(\text{Conformer 2}) > E(\text{Conformer 3})$  in the gas phase. The main issue for **Conformer 3** is that a rotation about the CH<sub>2</sub>-N<sub>3</sub> bond is necessary to achieve this special folded conformation and the activation energy may be high. These computations suggest that **9** may exist as a mixture of peptide conformations, likely in equilibrium.

Moreover, it is also possible that **Conformer 1** exhibits upward peptide branches interacting with each other, again by means of H-bonds. This is achieved by placing the peptidic branches at proximity to promote H-bond formations and start computations. At energy minimization,

dissymmetric conformations are systematically obtained sharing a common feature; the zinc(II)porphyrin chromophore is totally encapsulated. This situation is also considered. In order to assess whether the cavity formed by the peptides in **Conformation 1** is open or closed, bimolecular fluorescence oxidative quenching experiments are performed using C<sub>60</sub>, a well-known photo-oxidizing agent [19].

#### Effect of C<sub>60</sub> on the fluorescence lifetimes of **4**, **5**, **8** and **9**

The experiments were performed using the classic Stern-Volmer approach ( $\tau_F^0/\tau_F = 1 - k_{SV}[Q]$  with  $k_{SV} = \tau_F^0 \cdot k_Q$  with  $k_{SV}$  = Stern-Volmer quenching rate constant,  $k_Q$  = quenching rate constants,  $Q$  = quencher) [18]. A mixture of DMF (7%) and CCl<sub>4</sub> (93%) was used for solubility issues (C<sub>60</sub> is not soluble in DMF and **5** and **9** are not soluble in CCl<sub>4</sub>). The graph of the  $\tau_F^0/\tau_F$  vs. [C<sub>60</sub>] gives linear relationships for [Q]'s in the order of 10<sup>-6</sup> M, and the extracted  $k_{SV}$  and  $k_Q$  data are presented in Table 3. Knowing that **4**, **5**, and **8** exhibit perfectly accessible zinc(II)porphyrin chromophores for a C<sub>60</sub> approach, then any variation of the quenching rate constant would indicate either favorable or non-favorable interactions for electron transfer with the latter.

Indeed, evidence of fluorescence quenching was obtained for all four compounds, including **9** meaning that the zinc(II)porphyrin is accessible at all time. This experimental observation indicates that complete encapsulation of the central chromophore is not occurring. This is furthermore supported by the size of the  $k_Q$  (10<sup>13</sup> M<sup>-1</sup>.s<sup>-1</sup>) values indicating intermolecular association (*i.e.* close proximity) between the C<sub>60</sub> and the zinc(II) porphyrin central unit [20]. The similarity of the  $k_{SV}$  and  $k_Q$  values for **4** and **5** indicates similar driving forces for electron transfer and steric hindrance about the chromophore for C<sub>60</sub> intermolecular interactions (essentially none for both **4** and **5**). Both the  $k_{SV}$  and  $k_Q$  decrease by a factor of two going from **4** to **8**, but for unknown reasons. Sterically and electronically, **4** and **8** exhibit identical environment about the central chromophore and absorption and fluorescence maxima (Table 1). Nonetheless a decrease is observed and intrinsically a decrease in  $k_{SV}$

**Table 3.** Stern-Volmer ( $k_{SV}$ ) and fluorescence quenching rate constants for **4**, **5**, **8** and **9**<sup>a</sup>

Comp.	$\tau_F^0$ , ns	298 K (CCl <sub>4</sub> -7% DMF)	
		$k_{SV}$ , M <sup>-1</sup>	$k_Q$ , M <sup>-1</sup> .s <sup>-1</sup>
<b>4</b>	0.95	$5.7 \times 10^4$	$6.1 \times 10^{13}$
<b>5</b>	0.66	$4.6 \times 10^4$	$6.9 \times 10^{13}$
<b>8</b>	0.85	$2.9 \times 10^4$	$3.4 \times 10^{13}$
<b>9</b>	0.69	$1.0 \times 10^4$	$1.4 \times 10^{13}$

<sup>a</sup> The absorbance of each sample was adjusted at 0.15 at the 0-0 peak of the Q-bands.

and  $k_Q$  going from **5** to **9** is also expected. This is indeed observed (Table 3) but this decrease is by four fold. In overall, the large  $k_Q$  ( $10^{13} \text{ M}^{-1} \cdot \text{s}^{-1}$ ) is better explained by **9** existing as **Conformer 3**. This conclusion is consistent with the presence of a large amount of the non polar and aprotic solvent  $\text{CCl}_4$ . Indeed, in such a case, intramolecular H-bonds are favored, and therefore, **Conformer 3** is more likely to exist in this solvent. The four fold decrease in  $k_{SV}$  and  $k_Q$  means that interactions less favored and could mean that the more encumbered **Conformer 1** may be also in the solution hence explaining the slower rate. This would be consistent with the presence of 7% of DMF in the mixture that would be able to disrupt the intramolecular H-bonds and hence favoring **Conformer 1**. Because of solubility issues changing the relative amount of solvents was not possible as precipitation of one or the other was occurring. Similarly, measurements of IR spectra of **9** in solution were not possible due to strict solubility limitation.

## CONCLUSION

Using click chemistry, milligram scale of tetrasubstituted porphyrins **5** and **9** with peptides is rapidly and efficiently made and purified. The anchoring of oligopeptides onto the chromophore affects just a little the photophysical properties, except for some decreases consistent with the “loose bolt” effect. More importantly, the comparison of the bimolecular fluorescence quenching rate constants between **5** and **9** using  $\text{C}_{60}$  as a photo-oxidative agent provides evidence for some steric hindrance near the chromophore allowing one to suggest that **Conformer 3** is most likely the closest geometry of **9** in solution (93:7  $\text{CCl}_4/\text{DMF}$ ). In overall, this work demonstrates that models exhibiting pseudo protein environments are readily accessible. The choice of the appropriate peptides for solubility purposes (water or organic) is obviously an important issue for future works. Such works could include special pair models flanked with antennas similar to recent reports [21]. With the understanding that polypeptides are very polar residues greatly contributing to the stabilization of the charge separated state after the photo-induced electron transfer, the combination of this multi-peptide anchoring approach onto redox active porphyrins like hemes or related models and special pairs equipped with antennas should provide new model systems replicating better proteins such as myoglobin and the reaction center.

## Acknowledgements

PDH thanks the Natural Sciences and Engineering Research Council of Canada (NSERC), the Fonds Québécois de la Recherche sur la Nature et les Technologies (FQRNT), the Centre Québécois sur les Matériaux Fonctionnels (CQMF), and the Centre d'Excellence sur les Matériaux Optiques et Polymères de l'Université de Sherbrooke (CEMOPUS) for funding.

## REFERENCES

1. a) Hernandez-Eguia LP, Brea RJ, Castedo L, Ballester P and Granja JR. *Chem. Eur. J.* 2011; **17**: 1220–1229. b) Umezawa N, Matsumoto N, Iwama Sh, Kato N and Higuchi T. *Bioorg. Med. Chem.* 2010; **18**: 6340–6350. c) Carvalho IMM and Ogawa MY. *J. Braz. Chem. Soc.* 2010; **21**: 1390–1394. d) Bakleh M-E, Sol V, Granet R, Deleris G, Estieu-Gionnet K and Krausz P. *Chem. Comm.* 2010; **46**: 2115–2117. e) Jintoku H, Sagawa T, Sawada T, Takafuji M and Ihara H. *Org. Biomol. Chem.* 2010; **8**: 1344–1350. f) Setnicka V, Hlavacek J and Urbanova M. *J. Porphyrins Phthalocyanines* 2008; **12**: 1270–1278. g) Ikawa Y, Harada H, Toganoh M and Furuta H. *Bioorg. Med. Chem. Lett.* 2009; **19**: 2448–2452. h) Habdas J and Boduszek B. *J. Peptides Sci.* 2009; **15**: 305–311. i) Sol V, Chaleix V, Granet R and Krausz P. *Tetrahedron* 2008; **64**: 364–371. j) Wang J, Rosenblatt MM and Suslick KS. *J. Am. Chem. Soc.* 2007; **129**: 14124–14125.
2. a) Dmitriev RI, Ropiak HM, Yashunsky DV, Ponomarev GV, Zhdanov AV and Papkovsky DB. *FEBS J.* 2010; **277**: 4651–4661. b) Li Z-Y, Wang H-Y, Li C, Zhang X-L, Wu X-J, Qin S-Y, Zhang X-Z and Zhuo R-X. *J. Pol. Sci. A: Pol. Chem.* 2011; **49**: 286–292. c) Bourre L, Giuntini F, Eggleston IM, Mosse CA, MacRobert AJ and Wilson M. *Photochem. Photobiol.* 2010; **9**: 1613–1620. d) Dosselli R, Gobbo M, Bolognini E, Campestrini S and Reddi E. *ACS Med. Chem. Lett.* 2010; **1**: 35–38. e) Biron E and Voyer N. *Org. Biomol. Chem.* 2008; **6**: 2507–2515. f) Sibirian VM, Jensen TJ and Vicente MGH. *J. Med. Chem.* 2008; **51**: 2915–2923. g) Schroeder T, Schmitz K, Niemeier N, Balaban TS, Krug HF and Schepers UBS. *Biocon. Chem.* 2007; **18**: 342–354. h) Conway CL, Walker I, Bell A, Roberts DJH, Brown SB and Vernon DI. *Photochem. Photobiol.* 2008; **7**: 290–298. i) Habdas J and Boduszek B. *Hetero. Chem.* 2008; **19**: 107–111.
3. a) Ochiai T, Nagata M, Shimoyama K, Amano M, Kondo M, Dewa T, Hashimoto H and Nango M. *Langmuir* 2010; **26**: 14419–14422. b) Aziat F, Rein R, Peon J, Rivera E and Solladie N. *J. Porphyrins Phthalocyanines* 2008; **12**: 1232–1241. c) Ochiai T, Asaoka T, Kato T, Osaka S, Dewa T, Yamashita K, Gardiner AT, Hashimoto H and Nango M. *Photosyn. Research* 2008; **95**: 353–361. d) Hasobe T, Saito K, Kamat PV, Troiani V, Qiu H, Solladie N, Kim KS, Park JK, Kim D, D'Souza F and Fukuzumi S. *J. Mat. Chem.* 2007; **17**: 4160–4170. e) Hasobe T, Murata H, Fukuzumi S and Kamat PV. *Mol. Cryst. Liq. Cryst.* 2007; **471**: 39–51. f) Jintoku H, Sagawa T, Miyamoto K, Takafuji M and Ihara H. *Chem. Comm.* 2010; **46**: 7208–7210.
4. Zaytsev DV, Xie F, Mukherjee M, Bludin A, Demeler B, Breece RM, Tierney DL and Ogawa MY. *Biomacromol.* 2010; **11**: 2602–2609.

5. a) Maurer K, Grimm B, Wessendorf F, Hartnagel K, Guldi DM and Hirsch A. *Eur. J. Org. Chem.* 2010; 5010–5029. b) Kobata K, Ogawa J, Pandey SS, Oshima H, Arai T, Kato T and Nishino N. *Syn. Met.* 2007; **157**: 311–317.
6. Gnichwitz J-F, Wielopolski M, Hartnagel K, Hartnagel U, Guldi DM and Hirsch A. *J. Am. Chem. Soc.* 2008; **130**: 8491–8501.
7. Saito K, Troiani V, Qiu H, Solladié N, Sakata T, Mori H, Araki Y, Ito O and Fukuzumi S. *ECS Trans.* 2007; 157–165.
8. Krishnan V, Tronin A, Strzalka J, Fry HC, Therien MJ and Blasie JK. *J. Am. Chem. Soc.* 2010; **132**: 11083–11092.
9. Kuciauskas D and Caputo GA. *J. Phys. Chem. B* 2009; **113**: 14439–14447.
10. Fujitsuka M, Cho DW, Solladie N, Troiani V, Qiu H and Majima T. *J. Photochem. Photobiol. A* 2007; **188**: 346–350.
11. Ikawa Y, Harada H, Toganoh M and Furuta H. *Bioorg. Med. Chem. Lett.* 2009; **19**: 2448–2452.
12. a) Adrian R, McDonald NF, Gerard PM van K and Gerard van K. *J. Organomet. Chem.* 2009; **694**: 2153–2162. b) Li F, Yang SI, Ciringh Y, Seth J, Martin CH, Singh DL, Kim D, Birge RR, Bocian DF, Holten D and Lindsey JS. *J. Am. Chem. Soc.* 1998; **120**: 10001–10017.
13. Robey F and Fields RL. *Anal. Biochem.* 1989; **177**: 373–377.
14. Marik J and Sutcliffe JL. *Tet. Lett.* 2006; **47**: 6681–6684.
15. Egorova GD, Knyukshto VN, Solovev KN and Tsvirko MP. *Opt. Spektrosk.* 1980; **48**: 1101–1109.
16. Liu L, Fortin D and Harvey PD. *Inorg. Chem.* 2009; **48**: 5891–5900.
17. Harvey PD, Stern C and Guillard R. *Handbook of Porphyrin Science With Applications to Chemistry, Physics, Materials Science, Engineering, Biology and Medicine*, Kadish KM, Smith KM and Guillard R. (Eds.) World Scientific Publishing: Singapore, 2011; pp 1–179.
18. Turro, NJ, Ramamurthy V and Scaiano JC. *Modern Molecular Photochemistry of Organic Molecules*, University Science Books: Sausalito, California, 2010.
19. a) Imahori H and Sakata Y. *Eur. J. Org. Chem.* 1999; 24452–24457. b) Krasnov PO, Milyutina YM and Eliseeva NS. *Internet Elec. J. Mol. Design* 2010; **9**: 20–32. c) Basiuk VA. *J. Phys. Chem. A* 2005; **109**, 3704–3710.
20. D'Souza F, El-Khouly ME, Gadde S, McCarty AL, Karr PA, Zandler ME, Araki Y and Ito O. *J. Phys. Chem. B* 2005; **109**: 10107–10114.
21. a) Filatov M, Laquai F, Fortin D, Guillard R and Harvey PD. *Chem. Comm.* 2010; **48**: 9176–9178. b) Filatov MA, Guillard R and Harvey PD. *Org. Lett.*, 2010; **12**: 196–199.